

Supplementary Online Content

Posner J, Hellerstein DJ, Gat I, Mechling A, Klahr K, Wang, Z, McGrath PJ, Stewart JW, Peterson BS. Antidepressants normalize the default mode network in patients with dysthymia [published online February 6, 2013]. *JAMA Psychiatry*. doi:10.1001/jamapsychiatry.2013.455.

eAppendix 1. Summary of clinical trial

eAppendix 2. Functional connectivity analysis—imaging confounds

eAppendix 3. Negative control analysis

eAppendix 4. Network density

eAppendix 5. Baseline MRI scans: voxelwise comparison of duloxetine vs placebo arms

eAppendix 6. Baseline MRI scans: network comparison of duloxetine vs placebo arms

eAppendix 7. Comparison of participants who completed the study vs those who dropped out

eAppendix 8. Bootstrapping: differences in the sample sizes

eAppendix 9. Post hoc analyses of interaction detected in voxelwise analysis

eAppendix 10. Examining potential confounds in the network analysis

eAppendix 11. PCC-amygdalar connection strength correlations with depression symptom severity

eReferences

eFigure 1. Whole brain resting-state functional-connectivity maps with seed region in Brodmann area 4

eFigure 2. Whole brain resting-state functional connectivity map generated by comparing the baseline scans in the duloxetine vs placebo arms and the corresponding statistical output

eFigure 3. Comparison of the pretreatment and posttreatment scans

eTable 1. Default mode network regions

eTable 2. Duloxetine arm vs placebo arm

eTable 3. Connection strength with seed in the posterior cingulate cortex

eTable 4. Default mode network density

eTable 5. Baseline and posttreatment mean DMN densities

eTable 6. Comparison of posterior cingulate cortex connection strengths with other nodes in the default mode network in the pretreatment scans of the duloxetine and placebo study arms

This supplementary material has been provided by the authors to give readers additional information about their work.

eAppendix 1. Summary of Clinical Trial

A total of 65 DD participants enrolled in a 10-week double-blind, placebo-controlled study of duloxetine at the Depression Evaluation Service of the New York State Psychiatric Institute. A full description of the clinical trial is provided elsewhere¹. Of the 65 participants, N=60 were randomized and N=57 subjects provided data after the baseline visit. Of the 57 participants, based on intention-to-treat, the response rate was 65.5% (19/29) for duloxetine vs. 25.0% (7/28) for placebo (chi sq (df=1,n=57)= 9.43, p=.003); and remitter rate was 55.2% (16/29) for duloxetine vs. 14.3% (4/28) for placebo (chi sq (df=1,n=57)=10.46, p=.002). Of those who responded to active drug (n=19), 1 was taking 30 mg, 4 were taking 60 mg, 8 were taking 90 mg and 6 were taking 120 mg. Of those who responded to placebo (n=7), 0 were taking 30 mg, 1 was taking 60 mg, 1 was taking 90 mg, and 5 were taking 120 mg. For non-responders, those on placebo (n=21), 2 were taking 30 mg, 1 was taking 60 mg, 7 were taking 90 mg and 11 were taking 120 mg, while those on active drug (n=10), 1 was taking 30 mg, 3 were taking 60 mg, 2 were taking 90 mg, and 4 were taking 120 mg.

Patients who enrolled in the clinical trial were given the option of participating in the MRI study. Of these patients, N=46 consented to participant in the MRI study. In addition to these N=46 subjects, 5 additional subjects were recruited to add to the N of the MRI study. Therefore, there were a total of N=51 patients who consented to participate in the MRI study. Of these, we included N=41 in our MRI analyses. Thus N=10 subjects were not included for the following reasons: N=3 subjects had substantial

imaging artifacts that made analysis of their MRI data impossible; N=3 subjects requested that their MRI scan be stopped early due to discomfort in the scanner and thus no resting-state MRI data were collected; N=1 subject dropped out of the study prior to having an MRI scan done; N=1 subject was too large to fit into the bore of the magnet; N=1 subject disclosed taking medication on the day of the first MRI scan; and for N=1 subject, we were unable to acquire fMRI data due to technical problems with our MRI scanner.

In the clinical study, patients with Dysthymic Disorder (DD) as well as Depressive disorder NOS were included. The MRI study presented in the main text only included patients with a diagnosis of DD.

eAppendix 2. Functional Connectivity Analysis - Imaging

Confounds

Peripheral Physiology

Peripheral physiology, such as cardiac and respiratory cycles, influence fMRI signal intensity and can lead to overestimations of functional connectivity². Several methods are available to correct for these physiological effects³⁻⁵. We used a component-based noise reduction method, termed “CompCor”⁶. CompCor accounts for physiological effects by sampling BOLD signal from the brain’s white matter and ventricles. The time series data from these regions are included as nuisance regressors in the signal preprocessing procedures. CompCor is preferable to measuring physiological rhythms in the scanner, because by regressing fMRI signal from the brain’s white matter and the ventricles, CompCor accounts not only for physiological effects, but also for other sources of noise, such as head motion and signal drift^{3,5}. Regressing out the averaged whole brain fMRI signal is another approach to account for the untoward influence of peripheral physiology. We did not implement this approach, however, because regressing out mean whole brain fMRI signal can induce spurious anti-correlations of inter-regional fMRI signal². CompCor is as effective in accounting for the effects of peripheral physiology as the approach of mean whole brain regression, but without the risk inducing spurious anti-correlations³.

Head Motion

Recent work has shown that head motion, even micro-movements (i.e. movements $< 0.1\text{mm}$) during fMRI acquisition, can distort connectivity measures⁷. We took several steps to ensure that any group differences detected in connectivity were *not* the result of differential motion artifacts. First, we quantified head motion during the MRI scans. We calculated the root mean square (RMS) values of the adjustments needed to realign each participant's head position into the position that it was in at the beginning of each scanning run. We used a stringent cutoff of $< 1.5\text{ mm}$ RMS of motion per run, such that runs with $\geq 1.5\text{ mm}$ RMS motion would be excluded from the analyses. No runs met this cutoff criterion. Second, we tested whether head movement during the MRI scans differed between groups; very little RMS motion was detected (mean RMS values for healthy controls: 0.38mm ; baseline dysthymic participants subjects: 0.25mm ; post-treatment scan dysthymia arm: 0.26mm ; post-treatment scan placebo arm: 0.33mm) and *no* significant difference in head motion was found between groups. Third, during image processing, we attempted to correct for any motion effects by including nuisance regressors indexing the motion parameters along three axes and three rotations. Fourth, we included nuisance regressors indexing the first order derivatives of the motion parameters to account for the change in motion over time (i.e. the velocity of head motion).

eAppendix 3. Negative Control Analysis

To minimize the likelihood that our findings were the product of unspecified confounds or imaging artifacts, we conducted a control analysis by analyzing connectivity maps derived from a seed region within the primary motor cortex. We created this seed by averaging the fMRI signal across all voxels in Brodmann's area 4. In theory, motor system connectivity maps in dysthymic disorder (DD) and healthy control (HC) participants should be similar. Differences in motor system connectivity maps between DD and HC participants would suggest that confounding physiological, and/or other imaging artifacts, were biasing the data. Conversely, demonstrating no significant differences in the motor system connectivity maps in DD relative to HC participants would mitigate the probability that confounds were driving the study's main findings. We detected no group differences in the motor connectivity maps of DD and HC participants – see supplemental Figure 1.

eAppendix 4 - Network Density

Two principal approaches allow calculation of network density⁸ – valued and non-valued graphs. In the non-valued approach, each participant's correlation matrix is dichotomized, such that correlation coefficients are converted to 1's or 0's based on an investigator-determined threshold⁹. The investigator assigns a threshold for the correlation coefficients, above which the functional connections are interpreted as significant (and given a value of 1), and below which the functional connections are interpreted as insignificant (and given a value of 0). This generates a 12 x 12 correlation matrix, or graph, of 1's and 0's – a so-called, non-valued graph. Density in a non-valued graph is defined as the sum of all present connections divided by the sum of all possible connections¹⁰. This approach is conceptually parsimonious, but has significant limitations: a) the threshold by which the correlation coefficients are dichotomized is arbitrary, and b) information is sacrificed when the correlation coefficients are dichotomized (e.g., all correlation coefficients above the threshold are assigned the same value, 1, despite the fact that their true values may differ substantially). To circumvent these limitations, in a valued-graph, the values of the correlation coefficients are maintained in the matrix, and density is defined as the average of the correlation coefficients across the entire graph¹¹. This avoids the problems inherent in defining a threshold, but conversely, it includes functional connections with low correlation coefficients – connections that may be statistically insignificant. Given that both valued and non-valued graphical approaches each have shortcomings, we performed both. In

the main text, we present the valued graphical analyses; here, in the supplemental material, we present the non-valued graphical analyses. Because non-valued graphs require a threshold, we used multiple thresholds ranging between of $0.1 < z < 0.4$, to demonstrate that the findings were not threshold-dependent.¹² Irrespective of the threshold used, we found that the DMN density is consistently higher in the DD vs HC participants in the baseline scans (Supplemental Table 5A). Similarly, in the follow-up scans, we found a reduction in DMN density in the duloxetine arm but not in the placebo arm – this was true regardless of the threshold used (Supplemental Table 5B).

eAppendix 5 - Baseline MRI scans: Voxelwise Comparison of Duloxetine vs. Placebo Arms

Given the large number of statistical tests in a voxel-wise whole brain analysis, we reasoned that it was probable that baseline connectivity differences between the duloxetine and placebo arms could be present due to chance alone. These baseline differences in connectivity could produce spurious interpretations of treatment x time interactions. For example, baseline differences could include reduced connectivity in the placebo arm relative to the duloxetine arm. Following treatment, if the connectivity in the placebo and duloxetine became comparable, this change would be detected as an interaction (i.e. connectivity increased the placebo arm and decreased the duloxetine arm). However, we would not be able to determine what is driving this change. The interaction could be driven by placebo effect, duloxetine, or regression toward the mean. We reasoned that it was better to mask out voxels with baseline differences in connectivity rather than perform analyses that could yield ambiguous results.

To address baseline differences in connectivity, we compared the baseline MRI scans in the duloxetine vs. placebo arms by conducting an f-test on the PCC connectivity maps with a threshold of $p < 0.05$, no cluster size requirement. We used this liberal threshold to establish a conservative method for excluding baseline connectivity differences. The contrast image and statistical table derived from this analysis is presented in Supplemental Figure 2. We used the contrast image generated from this analysis as a mask to exclude from our interaction analyses any voxel in which there

were baseline differences in PCC connectivity between the duloxetine and placebo arms.

eAppendix 6 – Baseline MRI Scans: Network Comparison of Duloxetine vs Placebo Arms

As described in the Supplemental Text S5, baseline differences in connectivity between the duloxetine and placebo arms could produce spurious interpretation of treatment x time interactions. To negate this possibility in the network density analysis, we conducted an additional analysis focusing specifically on the DMN nodes. We isolated the functional connectivity of the PCC with each of the DMN nodes (listed in Supplemental Table 1). We then compared these connection strengths in the baseline scans from the duloxetine vs placebo groups (Supplemental Table 6). There was a significant difference between the duloxetine vs placebo groups in the PCC – Right Inferior Temporal Cortex connection (Supplemental Table 6). Voxels with baseline difference differences in connectivity were excluded from the voxelwise analysis – thus this baseline difference in PCC-Right Inferior Temporal Cortex connection strength should not have affected our results in the voxelwise analysis. However, this baseline difference in the PCC-Right Inferior Temporal Cortex connection strength could, in theory, affect the network analysis. To address this difference in baseline connectivity, we added this connection strength as a covariate in our network time by treatment interaction analysis. The treatment by time interaction remained statistically significant – for the related statistics, see Supplemental Text (S10).

eAppendix 7 – Comparison of Participants Who Completed the Study vs Those Who Dropped Out

Of the 41 patients who commenced the clinical trial and had their first MRI scan, nine dropped out of the study prior to completing the clinical trial and having their follow-up MRI scan. Of the N=9 dropouts, N=1 dropped out prior to being randomized and the other N=8 were equally distributed between the duloxetine (N=4) and placebo (N=4) arms. Comparison of those who completed the study vs. those who dropped out revealed that they were comparable on age ($t=0.3$; $p=0.8$) and gender (chi sq = 0.06, $p=0.8$)

eAppendix 8 – Bootstrapping: Differences in the Sample Sizes

The cohort of patients with DD was larger than the cohort of healthy controls (N=41 vs N=25). To test whether our finding of greater DMN connectivity in the DD group vs. the HC group was merely a product of the differences in sample sizes, we used bootstrapping to create 5000 random samples of 25 dysthymic patients to match the size of the control group. For each of the 5000 samples, we calculated the difference in the mean DMN connection density between DD and healthy control participants. In this way, we generated a 95% confidence interval around the mean difference in DMN connection density. The bootstrapped confidence interval (0.002 – 0.09) does not overlap with 0 and thus confirms our finding of greater DMN connectivity in the DD vs healthy control participants.

eAppendix 9 – Post-hoc Analyses of Interaction Detected in

Voxelwise Analysis

Voxelwise analysis of the DMN in the duloxetine and placebo arms demonstrated treatment by time interactions at the right lateral parietal cortex, right inferior temporal gyrus, and right middle to superior frontal cortex (Main Text - Table 3). To examine the nature of these interactions, we conducted the following post-hoc t-tests:

Comparison of the pre- and post-treatment scans demonstrated a treatment x time interaction in the connection between the posterior cingulate cortex (PCC) and the Right lateral parietal cortex ($F=7.3$, $p=0.01$). Specifically, the PCC-Right lateral parietal cortex connection was significantly lower in the post- vs pre-treatment scans in the duloxetine arm (Supplemental Figure 3; mean connection strength: 0.27 ± 0.2 vs. 0.54 ± 0.2 , $t=2.7$, $p=0.02$). The PCC-Right lateral parietal cortex connection strength differed significantly between pre-treatment duloxetine arm vs healthy controls (HCs) (Supplemental Figure 4; Mean connection strength pre-treatment: Duloxetine Arm= 0.54 ± 0.2 ; HCs= 0.28 ± 0.3 ; $t=3.6$; $p=0.001$). However, post-treatment the PCC-Right lateral parietal cortex connection strength was comparable between the duloxetine arm vs HCs (Supplemental Figure 3; Mean connection strength post-treatment: Duloxetine Arm= 0.27 ± 0.2 ; HCs= 0.28 ± 0.3 ; $t=0.1$; $p=0.9$). A similar treatment by time interaction was detected in the connection between the PCC and the Right inferior temporal gyrus ($F=10.8$, $p=0.003$). The PCC-Right inferior temporal cortex demonstrated a similar pattern of increased connectivity at baseline with normalization

following treatment (Supplemental Figure 3; Mean connection strength pre-treatment: Duloxetine Arm=0.26+/-0.1; HCs=0.07+/-0.2; $t=3.9$; $p<0.001$; Mean connection strength post-treatment: Duloxetine Arm=-0.02+/-0.2; HCs: 0.07+/-0.2; $t=1.6$; $p=0.1$).

For the Right mid-superior frontal cortex, the post-treatment connection strength was lower than the pre-treatment; however, with a two-tailed t-test, the change was not significant ($t=1.9$; $p=0.08$). Given that this was a post-hoc t-test following a significant omnibus f test, a one-sided t-test could arguably be appropriate, in which case the finding would be considered significant ($p=0.04$). Pre-treatment the Right mid-superior frontal cortex connection strength was comparable between the duloxetine arm vs HCs (Mean connection strength pre-treatment Duloxetine Arm=0.14+/-0.2; HCs: 0.17+/-0.2; $t=0.4$; $p=0.7$). Post-treatment the PCC-Right mid-superior frontal cortex connection strength was significantly lower in the Duloxetine arm vs HCs (Mean connection strength post-treatment: Duloxetine Arm= 0.02+/-0.1; HCs: 0.17+/-0.2; $t=2.3$; $p=0.03$). This suggests that duloxetine altered, but did not normalize, the PCC-Right mid-superior frontal cortex connection strength.

We conducted similar post-hoc testing in the placebo arm. The Right lateral parietal cortex and Right inferior temporal cortex connections did not show a significant change in connection strength between pre- and post-treatment (Right lateral parietal cortex: $t=0.6$; $p=0.6$; Right inferior temporal cortex connections: $t=-.06$; $p=0.9$) Conversely, we found that there was a significant increase in connection strength in the Right mid-superior frontal cortex between pre- and post-treatment ($t=2.6$; $p=0.02$).

eAppendix 10 – Examining Potential Confounds in the Network Analysis

In the main text, we examined the influence of treatment and time on DMN density in the duloxetine and placebo arms. While covarying for gender, we detected a treatment by time interaction $F(1,29)=5.0$; $p=0.03$). To ensure that this result was not driven by other potential confounds, we conducted additional analyses with: a) no covariates ($F(1,30) = 4.5$; $p=0.04$); b) covarying for gender ($F(1,29) = 5.0$; $p=0.03$); c) covarying for age ($F(1,29) = 4.4$; $p=0.04$); c) covarying for the number of days between the last day of the duloxetine clinical trial and the follow-up MRI scan ($F(1,27) = 5.5$; $p=0.03$); and d) covarying for a baseline difference in connectivity between the posterior cingulate cortex and the right inferior temporal cortex ($F(1,29) = 5.3$; $p=0.03$).

eAppendix 11 – PCC-amygdalar Connection Strength Correlations With Depression Symptom Severity

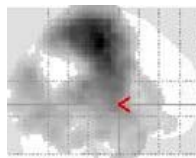
PCC-amygdalar connectivity no longer correlated with depressive symptom severity following treatment with either placebo or duloxetine. In the placebo arm, HAM-D scores obtained at the completion of the study did not correlate with the connection strength between the PCC and the left amygdala ($r=0.1$, $p=0.7$) or right amygdala ($r=-0.2$; $p=0.5$). Similarly, in the duloxetine arm, HAM-D scores obtained at the completion of the study did not correlate with the connection strength between the PCC and right amygdala ($r=-0.1$; $p=0.6$). In the duloxetine arm, HAM-D scores and the connection strength between the PCC and left amygdala demonstrated non-significant trend ($r=0.5$; $p=0.05$). We considered this non-significant because for the study's voxelwise analyses, the established alpha to control for multiple comparisons was 0.01.

eReferences:

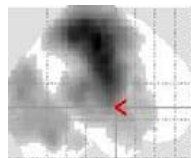
1. Hellerstein DJ, Stewart JW, McGrath P, Deliyannides D, Batchelder S, Black S, Withers A, O'Shea D, Chen Y. Duloxetine vs. placebo in treatment of chronic non-major depression. *Journal of Clinical Psychiatry*. in press.
2. Murphy K, Birn RM, Handwerker DA, Jones TB, Bandettini PA. The impact of global signal regression on resting state correlations: are anti-correlated networks introduced? *Neuroimage*. 2009;44(3):893-905.
3. Chai XJ, Castanon AN, Ongur D, Whitfield-Gabrieli S. Anticorrelations in resting state networks without global signal regression. *Neuroimage*. 2011.
4. Fox MD, Zhang D, Snyder AZ, Raichle ME. The global signal and observed anticorrelated resting state brain networks. *Journal of neurophysiology*. 2009;101(6):3270.
5. Weissenbacher A, Kasess C, Gerstl F, Lanzenberger R, Moser E, Windischberger C. Correlations and anticorrelations in resting-state functional connectivity MRI: a quantitative comparison of preprocessing strategies. *Neuroimage*. 2009;47(4):1408-1416.
6. Behzadi Y, Restom K, Liao J, Liu TT. A component based noise correction method (CompCor) for BOLD and perfusion based fMRI. *Neuroimage*. 2007;37(1):90-101.
7. Power JD, Barnes KA, Snyder AZ, Schlaggar BL, Petersen SE. Spurious but systematic correlations in functional connectivity MRI networks arise from subject motion. *Neuroimage*. 2011.
8. Butts CT. Social network analysis: A methodological introduction. *Asian Journal of Social Psychology*. 2008;11(1):13-41.
9. Doreian P. On the connectivity of social networks. *Journal of Mathematical Sociology*. 1974;3(2):245-258.
10. Sporns O. Graph theory methods for the analysis of neural connectivity patterns. *Neuroscience databases. A practical guide*. 2002:171-186.
11. Borgatti S, Everett M, Freeman L. *Ucinet for Windows: Software for Social Network Analysis*. Harvard, MA: Analytic Technologies; 2002.
12. Fair DA, Posner J, Nagel BJ, Bathula D, Dias TGC, Mills KL, Blythe MS, Giwa A, Schmitt CF, Nigg JT. Atypical default network connectivity in youth with attention-deficit/hyperactivity disorder. *Biol Psychiatry*. 2010.

eFigure 1: Whole brain resting-state functional connectivity maps with seed region in Brodmann's area 4. Qualitatively, the connectivity maps demonstrated the connectivity pattern of the motor cortex in both the dysthymic disorder (DD) participants (A) and in the healthy control (HC) participants (B). Comparison of the 2 groups (C) demonstrated no group differences in the motor connectivity maps of DD and HC participants

Supplemental Figure 1



A. Dysthymics



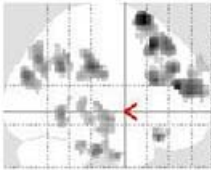
B. Controls



B. Dysthymics vs. Controls

eFigure 2: (A) Whole brain resting-state functional connectivity map generated by comparing the baseline scans in the duloxetine vs. placebo arms and (B) the corresponding statistical output. This analysis consisted of an f-test on the PCC connectivity maps comparing the baseline scans in the duloxetine vs. placebo arms with a threshold of $p < 0.05$, uncorrected. Some of clusters listed in the statistical output (B) are too small to clearly visualize on the connectivity map (A).

Supplemental Figure 2A



Supplemental Figure 2B

Statistics: p-values adjusted for search volume

set-level		cluster-level				peak-level					mm mm mm			
ρ	c	$\rho_{\text{FDR-adj}}$	$q_{\text{FDR-adj}}$	k_E	ρ_{uncorr}	$\rho_{\text{FDR-adj}}$	$q_{\text{FDR-adj}}$	F	(Z_{adj})	ρ_{uncorr}				
1.000	54			84		0.994	0.999	16.72	3.43	0.000	2	22	48	
				650		0.998	0.999	16.10	3.38	0.000	6	-32	30	
							1.000	0.999	12.66	3.02	0.001	6	-24	32
							1.000	0.999	11.48	2.88	0.002	6	-38	24
						309	0.999	0.999	15.41	3.31	0.000	18	14	66
							1.000	0.999	5.95	2.04	0.021	16	16	50
							1.000	0.999	4.93	1.83	0.033	12	22	46
						65	1.000	0.999	12.72	3.03	0.001	-32	-26	-32
						253	1.000	0.999	12.67	3.02	0.001	8	38	30
							1.000	0.999	12.64	3.02	0.001	6	24	22
							1.000	0.999	10.99	2.82	0.002	-2	20	22
						170	1.000	0.999	12.12	2.96	0.002	38	32	46
						147	1.000	0.999	11.70	2.91	0.002	28	50	12
							1.000	0.999	8.73	2.51	0.006	30	60	12
						67	1.000	0.999	11.41	2.87	0.002	40	-28	-34
							1.000	0.999	6.33	2.15	0.016	34	-40	-28
							1.000	0.999	5.76	2.00	0.023	20	-36	-26
						1	1.000	0.999	11.38	2.87	0.002	-38	-24	-36
						170	1.000	0.999	11.13	2.84	0.002	42	-84	28
							1.000	0.999	5.80	2.01	0.022	46	-74	16
						21	1.000	0.999	10.37	2.74	0.003	-48	-54	0

table shows 3 local maxima more than 8.0mm apart

Supplemental Figure 2B

Statistics: *p*-values adjusted for search volume

set-level		cluster-level				peak-level					mm mm mm		
ρ	c	$\rho_{\text{RUE}_{\text{out}}}$	$q_{\text{FDR}_{\text{out}}}$	k_E	ρ_{unout}	$\rho_{\text{RUE}_{\text{out}}}$	$q_{\text{FDR}_{\text{out}}}$	F	(Z_{p})	ρ_{unout}			
				103		1.000	0.999	10.03	2.70	0.004	14	-68	30
						1.000	0.999	5.53	1.96	0.025	14	-60	38
				100		1.000	0.999	9.60	2.64	0.004	-24	48	16
				374		1.000	0.999	9.32	2.60	0.005	68	-16	-8
						1.000	0.999	9.15	2.57	0.005	56	-18	-30
						1.000	0.999	7.87	2.38	0.009	72	-30	-8
				67		1.000	0.999	8.50	2.48	0.007	10	28	-20
				7		1.000	0.999	8.24	2.44	0.007	36	-24	10
				2		1.000	0.999	7.92	2.39	0.009	-42	-24	-36
				82		1.000	0.999	7.87	2.38	0.009	50	-54	30
				19		1.000	0.999	7.10	2.25	0.012	32	-70	32
						1.000	0.999	4.81	1.81	0.036	32	-74	40
				68		1.000	0.999	7.07	2.25	0.012	-26	32	32
						1.000	0.999	5.21	1.89	0.029	-32	30	38
				14		1.000	0.999	6.96	2.23	0.013	-18	-40	28
				15		1.000	0.999	6.86	2.21	0.014	-8	20	-22
				166		1.000	0.999	6.82	2.20	0.014	-36	-72	38
						1.000	0.999	6.17	2.08	0.019	-34	-66	32
						1.000	0.999	5.66	1.98	0.024	-38	-76	48
				27		1.000	0.999	6.78	2.20	0.014	-24	-40	-28
				22		1.000	0.999	6.76	2.19	0.014	-10	-78	42

table shows 3 local maxima more than 8.0mm apart

Supplemental Figure 2B

Statistics: *p*-values adjusted for search volume

set-level		cluster-level				peak-level					mm mm mm		
ρ	c	$\rho_{\text{RUE}_{\text{out}}}$	$q_{\text{FDR}_{\text{out}}}$	k_E	ρ_{unout}	$\rho_{\text{RUE}_{\text{out}}}$	$q_{\text{FDR}_{\text{out}}}$	F	(Z_{p})	ρ_{unout}			
				14		1.000	0.999	6.48	2.14	0.016	-30	6	68
				2		1.000	0.999	5.66	1.98	0.024	-26	8	70
				1		1.000	0.999	5.61	1.97	0.024	72	-38	4
				12		1.000	0.999	5.41	1.93	0.027	-18	46	50
				1		1.000	0.999	5.38	1.93	0.027	-8	38	-32
				7		1.000	0.999	5.35	1.92	0.027	66	-48	28
				27		1.000	0.999	5.34	1.92	0.027	-2	-70	20
				12		1.000	0.999	5.26	1.90	0.029	-8	72	4
				3		1.000	0.999	5.13	1.87	0.030	-24	-32	42
				21		1.000	0.999	5.05	1.86	0.032	-18	34	54
				7		1.000	0.999	5.04	1.85	0.032	14	-38	48
				16		1.000	0.999	5.03	1.85	0.032	-48	-64	20
				3		1.000	0.999	4.97	1.84	0.033	46	-12	-46
				5		1.000	0.999	4.92	1.83	0.034	-58	-60	40
				12		1.000	0.999	4.79	1.80	0.036	30	4	46
				1		1.000	0.999	4.77	1.80	0.036	-12	64	-14
				6		1.000	0.999	4.59	1.76	0.040	-34	24	-16
				4		1.000	0.999	4.59	1.75	0.040	2	70	-2
				1		1.000	0.999	4.54	1.75	0.040	-36	30	38
				1		1.000	0.999	4.47	1.73	0.042	-52	-66	16
				1		1.000	0.999	4.44	1.72	0.043	-18	34	48

table shows 3 local maxima more than 8.0mm apart

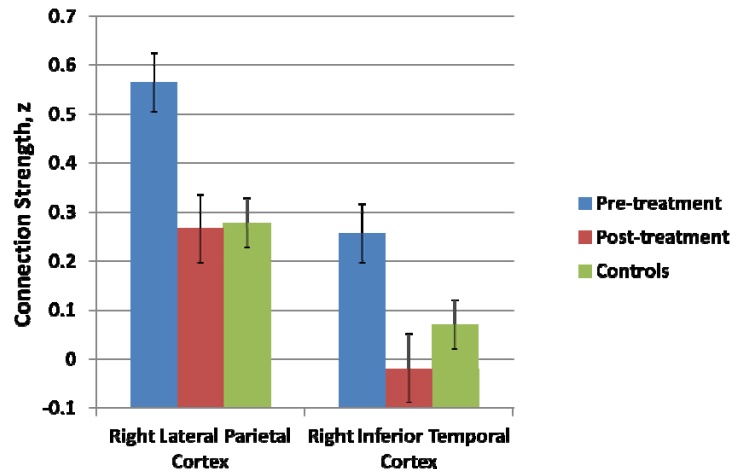
Supplemental Figure 2B

Statistics: *p*-values adjusted for search volume

set-level		cluster-level				peak-level				mm mm mm			
ρ	c	$\rho_{RJE_{\text{off}}}$	$q_{FDR_{\text{off}}}$	k_E	ρ_{unoff}	$\rho_{RJE_{\text{off}}}$	$q_{FDR_{\text{off}}}$	F	(Z_{off})	ρ_{unoff}			
				4		1.000	0.999	4.43	1.72	0.043	32	26	-18
				2		1.000	0.999	4.43	1.72	0.043	-8	72	0
				1		1.000	0.999	4.40	1.71	0.044	30	4	50
				1		1.000	0.999	4.31	1.69	0.046	-8	-60	22
				1		1.000	0.999	4.28	1.68	0.046	54	-48	30
				1		1.000	0.999	4.24	1.67	0.047	-12	72	0
				1		1.000	0.999	4.22	1.67	0.048	-34	-66	38
				1		1.000	0.999	4.20	1.66	0.048	-8	-60	26

eFigure 3: Comparison of the pre- and post-treatment scans demonstrated a treatment x time interaction in the connection between the posterior cingulate cortex (PCC) and the Right lateral parietal cortex ($F=7.3$, $p=0.01$). Specifically, the PCC-Right lateral parietal cortex connection was significantly lower in the post- vs pre-treatment scans in the duloxetine arm (mean connection strength: 0.54 ± 0.2 vs. 0.27 ± 0.2 , $t=2.7$, $p=0.02$). The PCC-Right lateral parietal cortex connection strength differed significantly between pre-treatment duloxetine arm vs healthy controls (HCs) (Mean connection strength pre-treatment: Duloxetine Arm= 0.54 ± 0.2 ; HCs= 0.28 ± 0.3 ; $t=3.6$; $p=0.001$). However, post-treatment the PCC-Right lateral parietal cortex connection strength was comparable between the duloxetine arm vs HCs (Mean connection strength post-treatment: Duloxetine Arm= 0.27 ± 0.2 ; HCs= 0.28 ± 0.3 ; $t=0.1$; $p=0.9$). A similar treatment by time interaction was detected in the connection between the PCC and the Right inferior temporal gyrus ($F=10.8$, $p=0.003$). The PCC-Right inferior temporal cortex demonstrated a similar pattern of increased connectivity at baseline with normalization following treatment (Mean connection strength pre-treatment: Duloxetine Arm= 0.26 ± 0.1 ; HCs= 0.07 ± 0.2 ; $t=3.9$; $p<0.001$; Mean connection strength post-treatment: Duloxetine Arm= -0.02 ± 0.2 ; HCs: 0.07 ± 0.2 ; $t=1.6$; $p=0.1$).

Supplemental Figure 3



eTable 1: Default Mode Network Regions

Regions	Abbreviations	Talairach Coordinates (x, y, z) from Fox et al.
Medial prefrontal cortex (ventral)	mPFC (ventral)	-3, 39, -2
Medial prefrontal cortex (anterior)	mPFC (anterior)	1, 54, 21
Posterior cingulate cortex	PCC	-2, -36, 37
Left lateral parietal cortex	L lat. parietal	-47, -67, 36
Right lateral parietal cortex	R lat. parietal	53, -67, 36
Left superior frontal cortex	L sup. frontal	-14, 38, 52
Right superior frontal cortex	R sup. frontal	17, 37, 52
Left inferior temporal cortex	L inf.temporal	-61, -33, -15
Right inferior temporal cortex	R inf.temporal	65, -17, -15
Left parahippocampal gyrus	L parahippocampus	-22, -26, -16
Right parahippocampal gyrus	R parahippocampus	25, -26, -14
Retrosplenial	Retrosplenial	3, -51, 8

eTable 2: Duloxetine Arm vs Placebo Arm

	Duloxetine Arm (N=15)	Placebo Arm (N=17)	Test statistic	p
Age in years (+/-SD)	38.0+/-9.7	38.1+/-9.2	t=0.02	0.9
Gender	Male=6 Female=9	Male=13 Female=4	X ² =4.4	0.04*
Hamilton Depression Summary Score (+/-SD)	20.7+/-3.6	20.9+/-3.7	t=0.2	0.9
Highest level of education	College or greater=9 High school=6 Below high school=0 Not specified=0	College or greater=11 High school=6 Below high school=0 Not specified=0	Mann Whitney U=121.5	0.8
Ethnicity/Race	Caucasian=10 African American=3 Hispanic=1 Asian=1 Not specified=0	Caucasian=15 African American=2 Hispanic=0 Asian=0 Not specified=0	X ² =3.1	0.4
Past or current anxiety disorder	N=6	N=7	X ² =0.005	0.9
Prior episode of MDD	N=4	N=5	X ² =0.03	0.9

* Statistically significant difference between the duloxetine and placebo arms.

eTable 3: Connection Strength With Seed in the Posterior Cingulate Cortex

Connection Strength with Seed in the Posterior Cingulate Cortex	MNI Coordinates			Cluster size	Peak t-value (z)	T-value with current anxiety disorders covaried	value with past anxiety disorders covaried	T-value with medication exposure covaried	T-value with MDD history covaried	T-value with substance abuse covaried	T-value with age covaried
	x	y	z								
Right Superior Frontal Cortex / Mesial Prefrontal Cortex	12	60	-8	193	2.95 (2.8)	2.89	2.55	3.84	3.32	2.8	3.1
Left Superior Frontal Cortex / Mesial Prefrontal Cortex	-14	66	4	103	3.08 (3.0)	2.73	3.09	2.9	2.33	2.6	3.3
Left lateral parietal cortex	-36	-90	22	266	3.20 (3.1)	2.69	2.97	3.54	2.95	2.9	3.3
Right lateral parietal cortex	48	-72	18	218	3.09 (3.0)	2.70	3.09	2.09	1.94	2.8	1.7
Precuneus	-8	-70	48	448	3.53 (3.4)	2.65	2.81	3.77	3.37	3.7	3.3

eTable 4: Default Mode Network Density

		DM N Den sity	Curre nt anxiet y disord ers covari ed (f, p)	Prior anxiet y disord ers covari ed (f, p)	Prior medic ation expos ure covari ed (f, p)	History of MDD covarie d (f, p)	Histor y of substa nce abuse covari ed (f, p)	Gend er Cova ried (f, p)	Age Cova ried (f, p)
Baseline Scans	Dysthymic Participants	0.23	4.65, 0.04	5.48, 0.02	5.9, 0.02	8.27, 0.005	5.23, 0.03	6.18, 0.02	9.4, 0.003
	Healthy Controls	0.17							

eTable 5: Baseline and Posttreatment Mean DMN Densities

A. Baseline - Mean DMN Densities		
Threshold	Healthy Controls	Dysthymics
0.1	0.67	0.84
0.15	0.42	0.62
0.2	0.3	0.41
0.25	0.17	0.29
0.3	0.13	0.23
0.35	0.08	0.18
0.4	0.05	0.12
B. Post-Treatment Mean DMN Densities		
Threshold	Duloxetine	Placebo
0.1	0.58	0.74
0.15	0.44	0.56
0.2	0.31	0.38
0.25	0.24	0.26
0.3	0.17	0.18
0.35	0.11	0.15
0.4	0.06	0.09

eTable 6: Comparison of Posterior Cingulate Cortex Connection Strengths With Other Nodes in the Default Mode Network in the Pre-treatment Scans of the Duloxetine and Placebo Study Arms

Regions	Duloxetine	Placebo	t	p
Medial prefrontal cortex (ventral)	0.25(0.2)	0.21(0.1)	0.7	0.5
Medial prefrontal cortex (anterior)	0.20(.3)	0.13(0.2)	0.7	0.5
Left lateral parietal cortex	0.39(0.3)	0.40(0.3)	0.1	0.9
Right lateral parietal cortex	0.48(0.3)	0.34(0.3)	1.2	0.2
Left superior frontal cortex	0.12(0.2)	0.14(0.3)	0.2	0.8
Right superior frontal cortex	0.23(0.3)	0.17(0.2)	0.7	0.5
Left inferior temporal cortex	0.19(0.3)	0.11(0.2)	0.9	0.4
Right inferior temporal cortex	0.34(0.2)	0.07(0.2)	4.1	0.001
Left parahippocampal gyrus	0.08(0.2)	0.14(0.2)	0.8	0.4
Right parahippocampal gyrus	0.10(0.2)	0.22(0.2)	1.5	0.1
Retrosplenial cortex	0.40(0.2)	0.44(0.3)	0.5	0.6